SINTEF
PROCEEDINGS
2

Proceedings of the 12th International Conference on Computational Fluid Dynamics in the Oil & Gas, Metallurgical and Process Industries

Progress in Applied CFD – CFD2017

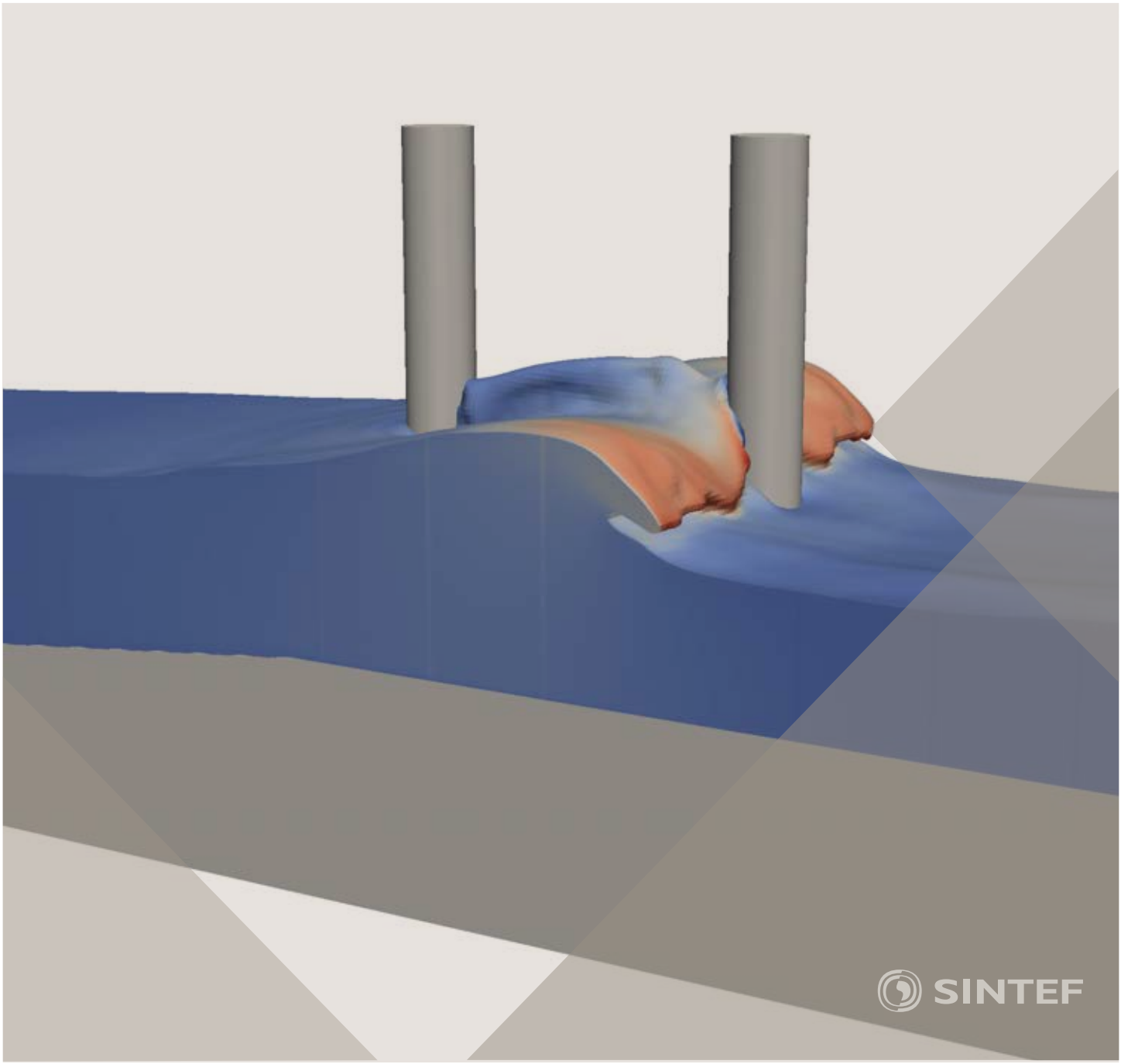

SINTEF Proceedings

Editors:
Jan Erik Olsen and Stein Tore Johansen

Progress in Applied CFD – CFD2017

Proceedings of the 12th International Conference on Computational Fluid Dynamics in the Oil & Gas, Metallurgical and Process Industries

SINTEF Academic Press

SINTEF Proceedings no 2
Editors: Jan Erik Olsen and Stein Tore Johansen
Progress in Applied CFD – CFD2017
Selected papers from 10th International Conference on Computational Fluid Dynamics in the Oil & Gas, Metallurgical and Process Industries

Key words:
CFD, Flow, Modelling

Cover, illustration: Arun Kamath

ISSN 2387-4295 (online)
ISBN 978-82-536-1544-8 (pdf)

SINTEF Academic Press
Address: Forskningsveien 3 B
PO Box 124 Blindern
N-0314 OSLO
Tel: +47 73 59 30 00
Fax: +47 22 96 55 08

www.sintef.no/byggforsk
www.sintefbok.no

SINTEF Proceedings
SINTEF Proceedings is a serial publication for peer-reviewed conference proceedings on a variety of scientific topics.
The processes of peer-reviewing of papers published in SINTEF Proceedings are administered by the conference organizers and proceedings editors. Detailed procedures will vary according to custom and practice in each scientific community.

PREFACE

This book contains all manuscripts approved by the reviewers and the organizing committee of the 12th International Conference on Computational Fluid Dynamics in the Oil & Gas, Metallurgical and Process Industries. The conference was hosted by SINTEF in Trondheim in May/June 2017 and is also known as CFD2017 for short. The conference series was initiated by CSIRO and Phil Schwarz in 1997. So far the conference has been alternating between CSIRO in Melbourne and SINTEF in Trondheim. The conferences focuses on the application of CFD in the oil and gas industries, metal production, mineral processing, power generation, chemicals and other process industries. In addition pragmatic modelling concepts and bio-mechanical applications have become an important part of the conference. The papers in this book demonstrate the current progress in applied CFD.

The conference papers undergo a review process involving two experts. Only papers accepted by the reviewers are included in the proceedings. 108 contributions were presented at the conference together with six keynote presentations. A majority of these contributions are presented by their manuscript in this collection (a few were granted to present without an accompanying manuscript).

The organizing committee would like to thank everyone who has helped with review of manuscripts, all those who helped to promote the conference and all authors who have submitted scientific contributions. We are also grateful for the support from the conference sponsors: ANSYS, SFI Metal Production and NanoSim.

Stein Tore Johansen & Jan Erik Olsen

Organizing committee:

Conference chairman: Prof. Stein Tore Johansen
Conference coordinator: Dr. Jan Erik Olsen
Dr. Bernhard Müller
Dr.Sigrid Karstad Dahl
Dr.Shahriar Amini
Dr.Ernst Meese
Dr.Josip Zoric
Dr.Jannike Solsvik
Dr.Peter Witt

Scientific committee:

Stein Tore Johansen, SINTEF/NTNU
Bernhard Müller, NTNU
Phil Schwarz, CSIRO
Akio Tomiyama, Kobe University
Hans Kuipers, Eindhoven University of Technology
Jinghai Li, Chinese Academy of Science
Markus Braun, Ansys
Simon Lo, CD-adapco
Patrick Segers, Universiteit Gent
Jiyuan Tu, RMIT
Jos Derksen, University of Aberdeen
Dmitry Eskin, Schlumberger-Doll Research
Pär Jönsson, KTH
Stefan Pirker, Johannes Kepler University
Josip Zoric, SINTEF

CONTENTS

12th International Conference on CFD in Oil & Gas, Metallurgical and Process Industries
SINTEF, Trondheim, NORWAY
May 30th - June 1st, 2017

NUMERICAL PREDICTIONS OF THE SHAPE AND SIZE OF THE RACEWAY ZONE IN A BLAST FURNACE

Dmitry SAFRONOV[1]*, **Andreas RICHTER**[1]†, **Bernd MEYER**[1]‡
[1]TU Bergakademie Freiberg, IEC, 09599 Freiberg, Germany

* E-mail: dmitry.safronov@vtc.tu-freiberg.de
† E-mail: a.richter@vtc.tu-freiberg.de
‡ E-mail: bernd.meyer@iec.tu-freiberg.de

ABSTRACT

A 3D transient numerical model has been developed to predict the shape and size of the raceway zone created by the force of the blast air injected through the tuyeres in the coke bed of a blast furnace. The model is based on the solution of conservation equations of both gas and solid phases as interpenetrating continua on an Eulerian-Eulerian frame of reference. A modified k-ε model has been adopted for gas phase turbulence including gas–coke turbulent interaction. The solid phase is characterized by the solid pressure, bulk viscosity and shear viscosity, which are evaluated by applying kinetic theory to granular flows. The influences of the air blast velocity, granular properties of the coke phase, and tuyere diameter on the shape and size of the raceway zone have been predicted by numerical simulations and described using semi-empirical relations. The effect of the cohesive zone on the raceway geometry is also taken into account. The trends of the derived results are compared with experimental data reported by various researchers with reasonable agreement.

Keywords: Process metallurgy, Ironmaking, Blast furnace, Raceway, CFD, Fluidized/packed beds, Granular flows.

NOMENCLATURE

Greek Symbols

α	Volume fraction, —
β	Momentum exchange coefficient, $\mathrm{kg\,m^{-3}\,s^{-1}}$
ε	Turbulent energy dissipation, $\mathrm{m^2\,s^{-3}}$
Θ	Granular temperature, K
μ	Dynamic (shear) viscosity, Pa s
ρ	Density, $\mathrm{kg\,m^{-3}}$
$\bar{\bar{\tau}}$	Stress tensor, Pa
ϕ	Angle of internal friction, degree
ξ	Bulk viscosity, Pa s

Latin Symbols

C_d	Drag coefficient, —
C_td	Turbulent dispersion coefficient, —
C_V	Added mass coefficient, —
D	Depth, m
d	Diameter, m
e	Coefficient of restitution, —
$\vec{F}$	Volume-specific force, $\mathrm{N\,m^{-3}}$
g_0	Radial distribution function, —
H	Height, m
$\vec{g}$	Standard acceleration due to gravity, $\mathrm{m\,s^{-2}}$
$\bar{\bar{I}}$	Unit tensor, —
k	Turbulent kinetic energy, $\mathrm{J\,kg^{-1}}$
L	Length, m
p	Pressure, Pa
Re	Reynolds number, —
$\vec{R}$	Interphase momentum exchange, $\mathrm{N\,m^{-3}}$
R_u	Universal gas constant, $\mathrm{J\,mol^{-1}\,K^{-1}}$
S	Cross-sectional area, $\mathrm{m^2}$
t	Time, s
T	Temperature, K
$\vec{U}$	Velocity, $\mathrm{m\,s^{-1}}$
$\dot{V}$	Volumetric flow, $\mathrm{m^3\,s^{-1}}$
W	Width, m

Sub/superscripts

0	Standard state
eff	Effective value
g	Gas phase
in	Inlet
i	Phase i
j	Phase j
max	Maximal value
rw	Raceway
s	Solid phase
t	Turbulent
td	Turbulent dispersion
tuyere	Tuyere

INTRODUCTION

The blast furnace (BF) that converts iron ore into molten iron is an important component in iron-steel making and a capital and energy intensive process. To maintain and improve the competitiveness of the blast furnace process, it is necessary to achieve a considerable decrease in the coke and total energy consumption for primary metal production along with minimization of environmental impacts. Injection of auxiliary fuels such as pulverized coal or oil has continuously made a considerable contribution toward reducing the requirement on expensive metallurgical coke in the last decades. The high coal injection rates and low coke rate is a common goal for reducing the cost of the hot metal production (Geerdes *et al.*, 2015). However, for an efficient and stable operation of the blast furnace towards increased injection rates, one has to understand the different physical processes and recognize the key parameters governing the processes.

In a blast furnace, iron-bearing materials and coke with flux are charged in alternate layers into the top of the furnace, as shown in Fig. 1. Preheated air and fuel (gas, oil or pulverized coal) are injected at high velocity into the lower part of the furnace through tuyeres, forming a cavity known as a raceway. In this raceway zone the injected fuel and some of the coke descending from the top of the furnace are combusted and gasified (see Fig. 2). The shape and size of the raceway greatly affect the conversion of the coke and the injected fuel.

In the previous decades, tremendous work had been conducted to investigate the kinetics of raceway formation. The works related to the prediction of the raceway size and shape can be classified into experimental, analytical, semi-empirical, and numerical types. Analytical and semi-empirical studies have considered dimensional analysis (Szekely and Poveromo, 1975; VDE, 1976; Flint and Burgess, 1992; Ohno *et al.*, 1994; Rajneesh *et al.*, 2004; Singh *et al.*, 2006; Gupta and Rudolph, 2006) or macroscopic mass and momentum balance above the raceway (Nomura, 1986) to find a correlation for the size of the raceway, which often was considered to be spherical or having other predefined simple geometrical shape. These works are often accompanied with experimental investigations of the raceway formation using simplified two- or three-dimensional physical models for determination of the modeling parameters.

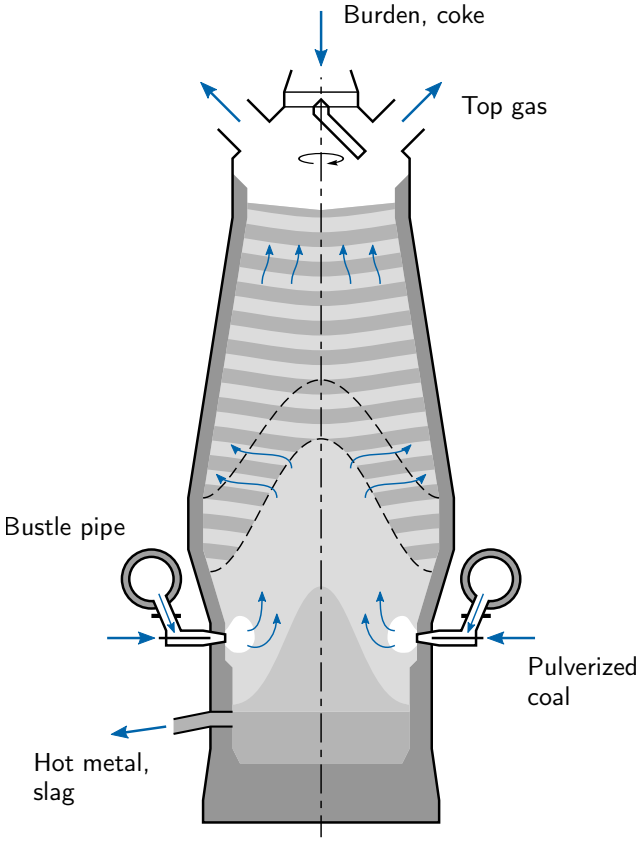

Figure 1: Ironmaking blast furnace (overview)

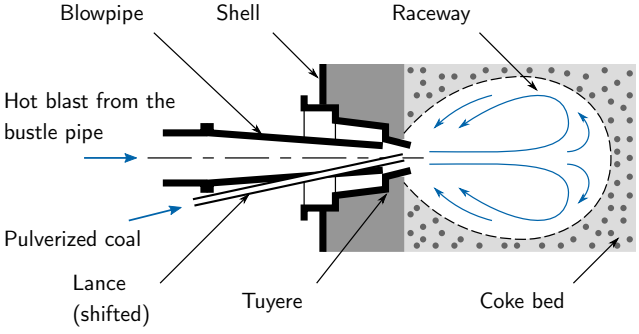

Figure 2: Coal injection in the raceway (tuyere level)

Numerical works can in turn be classifies into particle-resolved Discrete Element Modeling (DEM) and continuous Eulerial modeling. The literature shows that the DEM method has great potential but still has some significant challenges (Xu *et al.*, 2000; Nogami *et al.*, 2004; Yuu *et al.*, 2005; Hellberg *et al.*, 2005; Umekage *et al.*, 2007; Natsui *et al.*, 2011). All DEM models are significantly simplified, either by scaling up particles for industrial-scale furnaces, or scaled-down furnace size for real-size particles. This simplification lowers the computational load by reducing the number of particles. The geometry is further reduced in size by using a slot or thin pie-slice instead of the full cylindrical blast furnace shape, again reducing the number of particles in the simulation due to the high demand on computational resources.

In this work a comprehensive Eulerian approach is selected to describe the gas–coke particle flow. Aoki et al. (Aoki *et al.*, 1993) utilized the Eulerian approach to model the formation of raceway, but the authors neglected the effects of particles on gas phase turbulence in predicting the shape and size of the raceway zone. Mondal et al. (Mondal *et al.*, 2005) investigated the impact of coke bed and blast rates on the raceway shape and size applying Euler-Euler approach to a simplified two-dimensional BF geometry. More recently Selvarasu et al. (Selvarasu *et al.*, 2006, 2007) studied the raceway formation using geometry and operational parameters based on a real BF. However, no details on turbulent interaction between the gas and the solid phases can be found in the articles.

It has been recognized for many years that other blast furnace operation factors, such as the cohesive zone, arrangement of tuyeres and burden distribution also play an important role in the raceway formation and determine its size and shape. However, the effect of all those practical conditions on the raceway formation has not been studied very well. In order to improve our understanding of underlying physical processes, a three-dimensional Euler-Euler CFD model for simulation of the raceway formation process was developed. This work investigated the effect of tuyere geometry, air blast velocity, and coke particle size on the raceway formation. Possibilities to use the numerical predictions in real-time applications via reduced-order modeling approach are also discussed.

MODEL DESCRIPTION

Fig. 3 shows the geometry used in the simulations, which is based on the geometry of ArcelorMittal Eisenhüttenstadt BF 5A blast furnace. The computational domain consists of three tuyeres and includes the coke bed below the cohesive zone. The approximate shape and location of the cohesive zone is known from an analysis of vertical probing. The detailed size and shape of the deadman is dependent on the furnace inner profile and the shape and location of the cohesive zone.

Assumptions

The computational setup is based on the following basic assumptions:

- Coke particles are spheres of same size

- Particle collisions are considered as binary and inelastic
- Effect of fuel injection is not considered

Governing Equations

In the Eulerian approach, the different phases i are described mathematically as interpenetrating continua characterized by their volume fraction α_i. The volume fractions are assumed to be continuous functions of space and time and their sum is equal to one: $\sum_i \alpha_i = 1$. In this work two different phases are considered. The coke particles are represented by the solid granular phase and the blast air is referred as the gas phase. Momentum and continuity equations are obtained for each phase in terms of its volume fraction.
The continuity equation for phase i is

$$\frac{\partial(\alpha_i \rho_i)}{\partial t} + \nabla \cdot \left(\alpha_i \rho_i \vec{U}_i\right) = 0\,. \tag{1}$$

The momentum balance for phase i yields

$$\frac{\partial\left(\alpha_i \rho_i \vec{U}_i\right)}{\partial t} + \nabla \cdot \left(\alpha_i \rho_i \vec{U}_i \vec{U}_i\right) = - \alpha_i \nabla p_i + \nabla \cdot \bar{\bar{\tau}}_i + \alpha_i \rho_i \vec{g} + \vec{R}_{ij} + \vec{F}_{\mathrm{td},i}\,, \tag{2}$$

where $\bar{\bar{\tau}}_i$ is the stress-strain tensor for phase i

$$\bar{\bar{\tau}}_i = \alpha_i \mu_i \left(\nabla \vec{U}_i + \nabla \vec{U}_i^{\mathrm{T}}\right) + \alpha_i \left(\xi_i - \frac{2}{3}\mu_i\right) \nabla \cdot \vec{U}_i \bar{\bar{I}}, \tag{3}$$

with μ_i and ξ_i as the shear and bulk viscosities of phase i.
The interphase momentum exchange term $\vec{R}_{ij}$ describes the momentum transfer between the solid and the gas phase:

$$\vec{R}_{\mathrm{gs}} = \beta\left(\vec{U}_{\mathrm{g}} - \vec{U}_{\mathrm{s}}\right), \quad \vec{R}_{\mathrm{sg}} = \beta\left(\vec{U}_{\mathrm{s}} - \vec{U}_{\mathrm{g}}\right). \tag{4}$$

The interphase momentum exchange coefficient β was calculated according to the Gidaspow model (Gidaspow *et al.*, 1992), which is a combination of the Wen and Yu model (Wen and Yu, 1966) and the Ergun's equation (Ergun, 1952). For $\alpha_{\mathrm{g}} > 0.8$ the fluid–solid exchange coefficient β is based on the drag force of the fluid acting on a single particle:

$$\beta = \frac{3}{4} C_{\mathrm{d,s}} \frac{\alpha_{\mathrm{s}} \alpha_{\mathrm{g}} \rho_{\mathrm{g}} \left|\vec{U}_{\mathrm{s}} - \vec{U}_{\mathrm{g}}\right|}{d_{\mathrm{s}}} \alpha_{\mathrm{g}}^{-2.65} \tag{5}$$

and if $\alpha_{\mathrm{g}} \leq 0.8$, the exchange coefficient is described by Ergun's equation for dense granular systems as

$$\beta = 150 \frac{\alpha_{\mathrm{s}}^2 \mu_{\mathrm{g}}}{\alpha_{\mathrm{g}}^2 d_{\mathrm{s}}^2} + 1.75 \frac{\rho_{\mathrm{g}} \alpha_{\mathrm{s}} \left|\vec{U}_{\mathrm{s}} - \vec{U}_{\mathrm{g}}\right|}{\alpha_{\mathrm{g}} d_{\mathrm{s}}}. \tag{6}$$

The interphase drag coefficient $C_{\mathrm{d,s}}$ in Eqn. (5) is given by

$$C_{\mathrm{d,s}} = \frac{24}{\mathrm{Re}_{\mathrm{s}}} \left(1 + 0.15\,\mathrm{Re}_{\mathrm{s}}^{0.687}\right), \tag{7}$$

where the relative Reynolds number is defined as

$$\mathrm{Re}_{\mathrm{s}} = \frac{\rho_{\mathrm{g}} d_{\mathrm{s}} \left|\vec{U}_{\mathrm{s}} - \vec{U}_{\mathrm{g}}\right|}{\mu_{\mathrm{g}}}. \tag{8}$$

The turbulent dispersion force $\vec{F}_{\mathrm{td},i}$ in Eqn. (2) arises from averaging the interphase drag term $\vec{R}_{ij}$. For modeling of the turbulent dispersion force the formulation proposed by Lopez de Bertodano (de Bertodano, 1991) was used:

$$\vec{F}_{\mathrm{td,g}} = -\vec{F}_{\mathrm{td,s}} = C_{\mathrm{td}} \rho_{\mathrm{g}} k_{\mathrm{g}} \nabla \alpha_{\mathrm{s}}\,, \quad C_{\mathrm{td}} = 1 \tag{9}$$

The bulk viscosity of the gas phase is considered to be zero

$$\xi_{\mathrm{g}} = 0 \tag{10}$$

and the effective dynamic viscosity (shear viscosity) is calculated from the molecular and turbulent viscosities as follows:

$$\mu_{\mathrm{eff,g}} = \mu_{\mathrm{g}} + \mu_{\mathrm{t,g}}\,. \tag{11}$$

The turbulent viscosity, $\mu_{\mathrm{t,g}}$, is modeled by modified k-ε closure equations for turbulence

$$\mu_{\mathrm{t,g}} = \rho_{\mathrm{g}} C_{\mu} \frac{k_{\mathrm{g}}^2}{\varepsilon_{\mathrm{g}}}, \tag{12}$$

where the turbulent kinetic energy, k_{g}, and turbulent kinetic energy dissipation rate, ε_{g}, are determined from their respective conservation equations (13) and (14) considering the effect of solid particles.

$$\frac{\partial\left(\alpha_{\mathrm{g}} \rho_{\mathrm{g}} k_{\mathrm{g}}\right)}{\partial t} + \nabla \cdot \left(\alpha_{\mathrm{g}} \rho_{\mathrm{g}} \vec{U}_{\mathrm{g}} k_{\mathrm{g}}\right) = \nabla \cdot \left(\alpha_{\mathrm{g}} \frac{\mu_{\mathrm{t,g}}}{\sigma_k} \nabla k_{\mathrm{g}}\right) + \alpha_{\mathrm{g}} G_{k,\mathrm{g}} - \alpha_{\mathrm{g}} \rho_{\mathrm{g}} \varepsilon_{\mathrm{g}} + \underbrace{\beta\left(k_{\mathrm{sg}} - 2k_{\mathrm{g}}\right)}_{\text{phase interaction}}, \tag{13}$$

$$\frac{\partial\left(\alpha_{\mathrm{g}} \rho_{\mathrm{g}} \varepsilon_{\mathrm{g}}\right)}{\partial t} + \nabla \cdot \left(\alpha_{\mathrm{g}} \rho_{\mathrm{g}} \vec{U}_{\mathrm{g}} \varepsilon_{\mathrm{g}}\right) = \nabla \cdot \left(\alpha_{\mathrm{g}} \frac{\mu_{\mathrm{t,g}}}{\sigma_{\varepsilon}} \nabla \varepsilon_{\mathrm{g}}\right) + \alpha_{\mathrm{g}} \frac{\varepsilon_{\mathrm{g}}}{k_{\mathrm{g}}} \left(C_{1\varepsilon} G_{k,\mathrm{g}} - C_{2\varepsilon} \rho_{\mathrm{g}} \varepsilon_{\mathrm{g}}\right) + \underbrace{C_{3\varepsilon} \frac{\varepsilon_{\mathrm{g}}}{k_{\mathrm{g}}} \beta\left(k_{\mathrm{sg}} - 2k_{\mathrm{g}}\right)}_{\text{phase interaction}}. \tag{14}$$

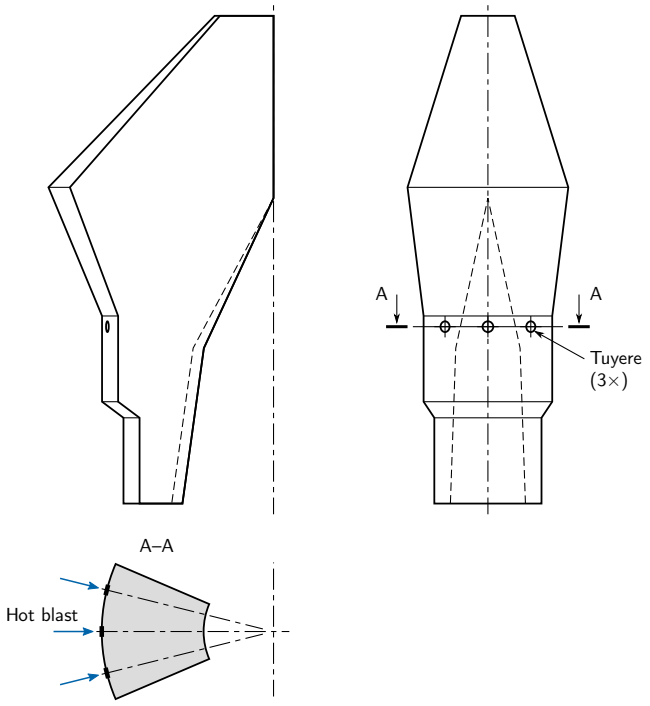

Figure 3: Computational domain for the raceway simulation

$G_{k,\mathrm{g}}$ in Eqn. (13) is the production of turbulent kinetic energy in the gas phase. The last term in both the equations represents the influence of the dispersed phases (solid phase) on the continuous phase (Elgobashi and Abou, 1983). The constants for the k-ε model are (Launder and Spalding, 1972, 1974; Ferziger and Perić, 2002)

$$C_\mu = 0.09\,, \quad C_{1\varepsilon} = 1.44\,, \quad C_{2\varepsilon} = 1.92\,, \quad C_{3\varepsilon} = 1.2\,, \quad \sigma_k = 1.0\,, \quad \sigma_\varepsilon = 1.3\,. \tag{15}$$

The term k_{sg} in Eqn. (13) and (14) is the covariance of the velocities of the continuous phase and the solid phase (Simonin and Viollet, 1990) and is given by

$$k_{\mathrm{sg}} = 2\,k_{\mathrm{g}} \left(\frac{b+\eta_{\mathrm{sg}}}{1+\eta_{\mathrm{sg}}} \right), \tag{16}$$

where the term b can be expressed as

$$b = (1+C_{\mathrm{V}}) \left(\frac{\rho_{\mathrm{s}}}{\rho_{\mathrm{g}}} + C_{\mathrm{V}} \right)^{-1} \tag{17}$$

with $C_{\mathrm{V}} = 0.5$ as added-mass coefficient.
The term η_{sg} can be written as the ratio of the Lagrangian integral time scale and the characteristic particle relaxation time scale as

$$\eta_{\mathrm{sg}} = \frac{\tau_{\mathrm{t,\,sg}}}{\tau_{\mathrm{F,\,sg}}}\,. \tag{18}$$

The characteristic particle relaxation time scale connected with inertial effects acting on a dispersed phase is defined as

$$\tau_{\mathrm{F,\,sg}} = \alpha_{\mathrm{s}}\,\rho_{\mathrm{s}}\,\beta^{-1} \left(\frac{\rho_{\mathrm{s}}}{\rho_{\mathrm{g}}} + C_{\mathrm{V}} \right). \tag{19}$$

The eddy particle interaction time is mainly affected by the crossing-trajectory effect (Csanady, 1963) and defined as

$$\tau_{\mathrm{t,\,sg}} = \frac{\tau_{\mathrm{t,\,g}}}{\sqrt{\left(1+C_\beta\,\xi^2\right)}}\,, \tag{20}$$

where

$$\xi = \frac{\left|\vec{U}_{\mathrm{sg}}\right| \tau_{\mathrm{t,\,g}}}{L_{\mathrm{t,\,g}}} \tag{21}$$

and

$$C_\beta = 1.8 - 1.35\cos^2\theta\,. \tag{22}$$

θ is the angle between the mean particle velocity $\vec{U}_{\mathrm{s}}$ and the mean relative velocity $\vec{U}_{\mathrm{sg}}$.
The time scale of the energetic turbulent eddies appearing in Eqn. (20) is defined as

$$\tau_{\mathrm{t,\,g}} = \frac{3}{2}\,C_\mu\,\frac{k_{\mathrm{g}}}{\varepsilon_{\mathrm{g}}} \tag{23}$$

and the length scale of the turbulent eddies appearing in Eqn. (21) is given by

$$L_{\mathrm{t,\,g}} = \sqrt{\frac{3}{2}}\,C_\mu\,\frac{k_{\mathrm{g}}^{3/2}}{\varepsilon_{\mathrm{g}}}\,. \tag{24}$$

The solid phase is characterized by the solid pressure, bulk viscosity and shear viscosity, which are evaluated by applying kinetic theory to granular flows. All the three quantities, namely, p_{s}, ξ_{s}, and μ_{s}, arise from the momentum transport due to the movement and interaction (translation, collision, and friction) of coke particles.

The solids pressure represents the particle normal forces (Gidaspow, 1994; Gidaspow *et al.*, 1992; Huilin *et al.*, 2003; Ding and Gidaspow, 1990) and is composed of a kinetic term and a second term due to particle collisions:

$$p_{\mathrm{s}} = \alpha_{\mathrm{s}}\,\rho_{\mathrm{s}}\,\Theta_{\mathrm{s}} + 2\,\rho_{\mathrm{s}}\,(1+e_{\mathrm{ss}})\,\alpha_{\mathrm{s}}^2\,g_{0,\mathrm{ss}}\,\Theta_{\mathrm{s}}\,, \tag{25}$$

where e_{ss} is the coefficient of restitution for particle collisions, Θ_{s} is the granular temperature, and $g_{0,\mathrm{ss}}$ is the radial distribution function.

The distribution function $g_{0,\mathrm{ss}}$ describes the transition from the "compressible" condition ($\alpha_{\mathrm{s}} < \alpha_{\mathrm{s,max}}$), where the spacing between the solid particles can continue to decrease, to the "incompressible" one, where no further decrease in the spacing is possible:

$$g_{0,\mathrm{ss}} = \frac{3}{5}\left[1 - \left(\frac{\alpha_{\mathrm{s}}}{\alpha_{\mathrm{s,max}}}\right)^{1/3}\right]^{-1}, \tag{26}$$

where $\alpha_{\mathrm{s,max}}$ is the packing limit for the solid phase.

The granular temperature Θ_{s} is proportional to the kinetic energy of the fluctuating particle motion. The energy transport equation for the solid granular phase in terms of granular temperature Θ_{s} derived from kinetic theory takes the form (Gidaspow *et al.*, 1992; Ding and Gidaspow, 1990):

$$\frac{3}{2}\frac{\partial\left(\rho_{\mathrm{s}}\,\alpha_{\mathrm{s}}\,\Theta_{\mathrm{s}}\right)}{\partial t} + \frac{3}{2}\nabla\cdot\left(\rho_{\mathrm{s}}\,\alpha_{\mathrm{s}}\,\vec{U}_{\mathrm{s}}\Theta_{\mathrm{s}}\right) = \bar{\bar{\tau}}_{\mathrm{s}}:\,\nabla\vec{U}_{\mathrm{s}} + \nabla\cdot\left(k_{\Theta_{\mathrm{s}}}\,\nabla\Theta_{\mathrm{s}}\right) - \gamma_{\Theta_{\mathrm{s}}} - 3\,\beta\,\Theta_{\mathrm{s}}\,, \tag{27}$$

where the first term on the right-hand side represents the generation of energy by the solid stress tensor, the second term represents the diffusion of energy, the third term represents the collisional dissipation of energy and the last term represents the exchange of kinetic energy from the solid phase to the gas phase.

The diffusion coefficient $k_{\Theta_{\mathrm{s}}}$ and collisional dissipation of granular energy $\gamma_{\Theta_{\mathrm{s}}}$ in Eqn. (27) can be expressed (Gidaspow *et al.*, 1992; Huilin *et al.*, 2003; Ding and Gidaspow, 1990) as

$$k_{\Theta_{\mathrm{s}}} = \frac{150\,\rho_{\mathrm{s}}\,d_{\mathrm{s}}\sqrt{\Theta_{\mathrm{s}}\,\pi}}{384\,(1+e_{\mathrm{ss}})\,g_{0,\mathrm{ss}}}\left[1+\frac{6}{5}\,g_{0,\mathrm{ss}}\,\alpha_{\mathrm{s}}\,(1+e_{\mathrm{ss}})\right]^2 + 2\,\alpha_{\mathrm{s}}^2\,\rho_{\mathrm{s}}\,d_{\mathrm{s}}\,g_{0,\mathrm{ss}}\,(1+e_{\mathrm{ss}})\left(\frac{\Theta_{\mathrm{s}}}{\pi}\right)^{1/2}, \tag{28}$$

$$\gamma_{\Theta_{\mathrm{s}}} = 3\left(1-e_{\mathrm{ss}}^2\right)g_{0,\mathrm{ss}}\,\rho_{\mathrm{s}}\,\alpha_{\mathrm{s}}^2\,\Theta_{\mathrm{s}} \times \left[\frac{4}{d_{\mathrm{s}}}\left(\frac{\Theta_{\mathrm{s}}}{\pi}\right)^{1/2} - \nabla\cdot\vec{U}_{\mathrm{s}}\right]. \tag{29}$$

The shear viscosity and bulk viscosity appearing in Eqn. (3) for the solid granular phase can be written (Gidaspow, 1994; Gidaspow *et al.*, 1992; Huilin *et al.*, 2003; Ding and Gi-

daspow, 1990; Schaffer, 1987; Lun *et al.*, 1984) as

$$\mu_s = \underbrace{\frac{4}{5}\alpha_s^2 \rho_s d_s g_{0,ss} (1+e_{ss}) \left(\frac{\Theta_s}{\pi}\right)^{1/2}}_{\text{collisional part}} + \underbrace{\frac{10\rho_s d_s \sqrt{\Theta_s \pi}}{96(1+e_{ss}) g_{0,ss}} \left[1+\frac{4}{5} g_{0,ss} \alpha_s (1+e_{ss})\right]^2}_{\text{kinetic part}} + \underbrace{\frac{p_s \sin\phi_s}{2\sqrt{I_{2D}}}}_{\text{frictional part}}, \quad (30)$$

$$\xi_s = \frac{4}{3}\alpha_s^2 \rho_s d_s g_{0,ss} (1+e_{ss}) \left(\frac{\Theta_s}{\pi}\right)^{1/2}, \quad (31)$$

where ϕ_s is the angle of internal friction for the solid phase, p_s is the solid pressure, and I_{2D} is the second invariant of the deviatoric stress tensor.

CFD SETUP AND VALIDATION

The conservation equations for the gas and the solid phase were solved using an implicit Finite Volume Method (FVM). A coupling between the pressure and velocity was accomplished using the Phase Coupled SIMPLE (PC-SIMPLE) algorithm for the pressure–velocity coupling. The velocities are solved coupled by phases, but in a segregated fashion. Pressure and velocities are then corrected by solving a pressure correction equation to satisfy the continuity constraint. The space derivatives of the diffusion terms were discretized by a central differencing scheme, while the advection terms were discretized by a power law scheme.

The computational domain consists of approximately 10^6 control volumes after a grid sensitivity study. At the hot blast inlet, the air velocity was considered to be uniform and the volume fraction of gas was unity ($\alpha_{g,in} = 1$). The pressure was definded at the outlet and the axial gradients of all other variables were set to zero. In order to specify the pressure at the outlet of the computational domain, the effect of assumed burden distribution was modeled separately using the full BF inner profile and considering the pressure drop due to the cohesive zone measured by a vertical probing. Turbulent quantities k and ε in the near-wall cells were prescribed from a logarithmic wall function. Symmetric boundary conditions (normal gradient is zero) were applied at the side walls. A no-slip condition was set at the wall for the gas phase calculations. The solid normal velocity was also set to zero at the wall. The burden properties used in the calculations are summarized in Table 1.

The validity of the computational model is examined using the data reported by Nomura for Newcasle No. 1 BF in Australia (Nomura, 1986). The conditions used for the validation are listed in Table 2. Fig. 4 shows the comparison in the raceway depth L_{rw} between CFD simulation results and the experimental results. It can be seen that the CFD model is in reasonable agreement with experimental work and is also able to predict actual physical trends accurately and within acceptable limits.

SIMULATION CONDITIONS

The various conditions for the parametric studies are shown in Table 3. These parameters are collected from an actual operation case.

Table 1: Granulometric and mechanic properties of the granular phase (Adema, 2014; Natsui *et al.*, 2011; Yuu *et al.*, 2010)

Parameter	Coke	Ore
Particle size	38 mm	38 mm
Particle density	1100 kg m^{-3}	4000 kg m^{-3}
Volumetric fraction in the burden above cohesive zone	0.4	0.6
Volumetric fraction in the burden below cohesive zione	1.0	0.0
Shear modulus	10^7 Pa	10^7 Pa
Coefficient of restitution	0.8	0.8
Angle of internal friction	45°	45°
Packing limit $\alpha_{s,max}$	0.63	0.63

Table 2: Validation conditions

Tuyere diameter	152 mm
Coke particle size	41–49 mm
Blast velocity	90–120 m s^{-1}
Blast temperature	973 K

RESULTS

Figs. 5 and 6 show the distribution of the volume fraction of the solid phase α_s in the region near tuyeres. A macroscopically stable raceway is formed in front of the tuyere under the combined effect of the gas flow and the motion of the solid particles. The boundary of the raceway zone separating it from the coke bed is characterized by the lines of constant volume fraction which is equal to the initial volume fraction of solid, α_s. The raceway is characterized by a central high void region and circulating particle region near the raceway boundary. Although the boundary may show some fluctuation, the overall raceway size remains almost unchanged. The blast air incurs a relatively large momentum exchange with the solid phase in the radial direction and results in convecting the solid particles radially towards the furnace axis. Through the momentum exchange the air flow loses its kinetic energy and is predominantly moving upward as expected (see Fig. 7).

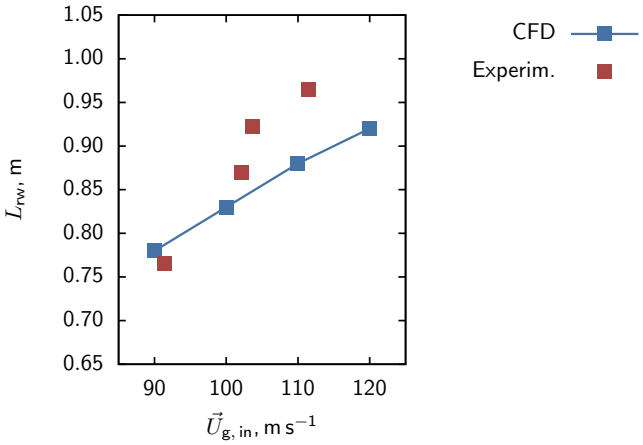

Figure 4: Comparison in the raceway depth L_{rw} between CFD simulation results and experimental data reported by Nomura (Nomura, 1986)

Table 3: Operating conditions

Tuyere diameter	123 mm
Tuyere angle	4°
Coke particle size	25–38 mm
Blast velocity	140–300 m s^{-1}
Blast temperature	1413 K

The velocity distribution inside the raceway is an important factor that decides the conversion behavior of the coke and injected fuels. Fig. 8 shows the streamlines of the gas phase inside the raceway and in the surrounding coke bed. At the top and bottom of the raceway near the wall of the furnace stagnation zones can be observed. Their existence can also be verified by some particle-resolved simulations (Hilton and Cleary, 2012). In the middle of the raceway a recirculation area is formed. This area defines the extent of the raceway and influences the residence time of the injected fuel particles.

The effect of the blast velocity is shown in Fig. 9, 10, and 11. The raceway size increases as the tuyere velocity rises. An increase in the gas velocity increases the momentum of the gas phase, which in turn causes a larger momentum exchange with the solid particles, moving them further away from the tuyere towards the center of the furnace. The raceway is larger for a higher tuyere velocity. It is also observed that the interaction between the different raceways increases with the increased tuyere velocity.

The effect of coke particle size is shown in Fig. 12. The results show that the raceway size increases as the coke size decreases, because smaller particles have larger specific surface area and gains stronger drag force from the gas flow with respect to their weight. This is in agreement with various experimental observations and correlations (Rajneesh *et al.*, 2004; Gupta, 2005; Gupta and Rudolph, 2006), where it is observed that the raceway shape is inversely proportional

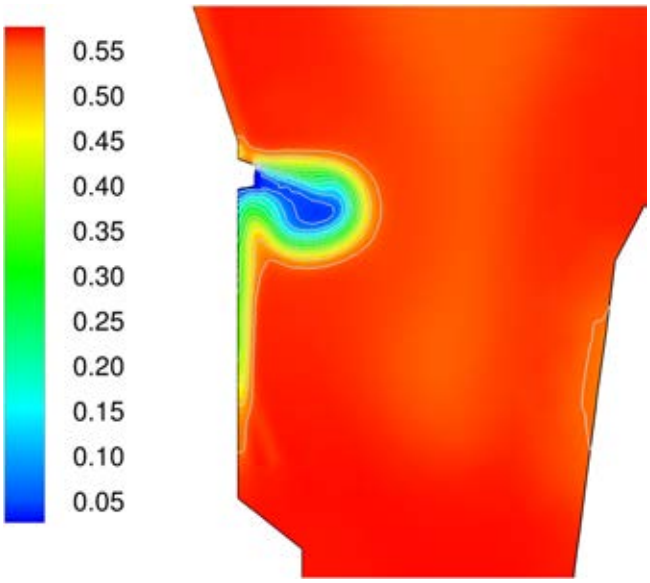

Figure 5: Spatial distribution of the granular phase volume fraction α_s for the inlet velocity $\vec{U}_{g,in} = 230\,\mathrm{m\,s^{-1}}$ and the coke particle size $d_s = 0.038\,\mathrm{m}$ (axial cross-section)

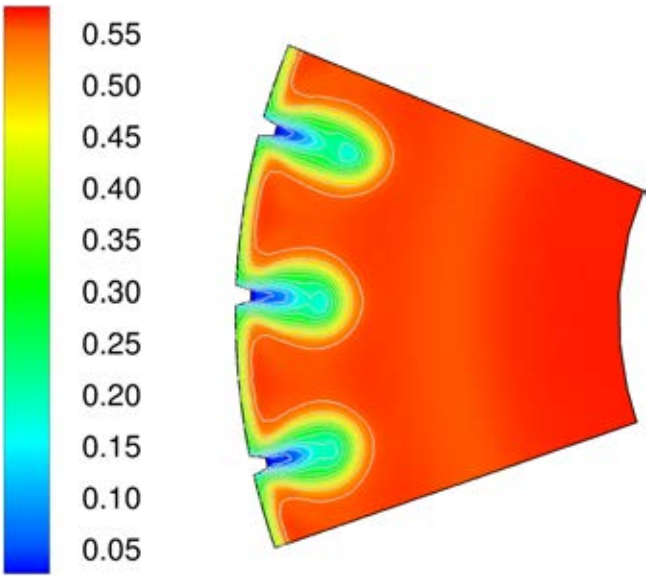

Figure 6: Spatial distribution of the granular phase volume fraction α_s for the inlet velocity $\vec{U}_{g,in} = 230\,\mathrm{m\,s^{-1}}$ and the coke particle size $d_s = 0.038\,\mathrm{m}$ (tuyere level)

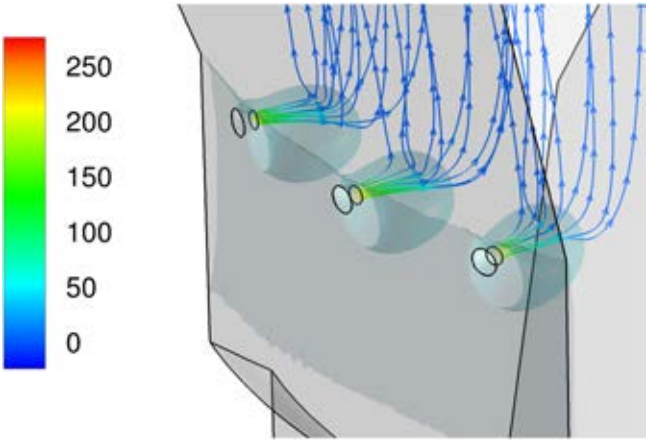

Figure 7: Streamlines of the gas phase colored by the gas velocity $\vec{U}_g$ ($\mathrm{m\,s^{-1}}$) and iso-surfaces of the granular phase volume fraction α_s (filled) for the inlet velocity $\vec{U}_{g,in} = 230\,\mathrm{m\,s^{-1}}$ and the coke particle size $d_s = 0.038\,\mathrm{m}$

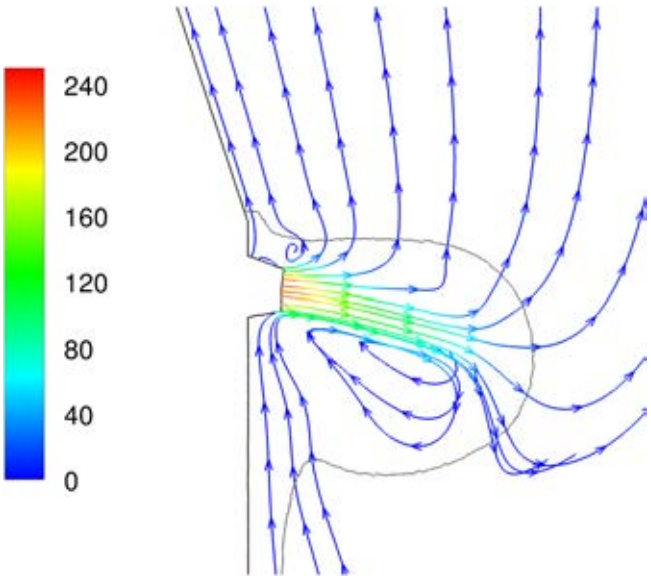

Figure 8: Streamlines of the gas phase colored by the gas velocity $\vec{U}_g$ ($\mathrm{m\,s^{-1}}$) for the inlet velocity $\vec{U}_{g,in} = 230\,\mathrm{m\,s^{-1}}$ and the coke particle size $d_s = 0.038\,\mathrm{m}$ (axial cross-section)

to the coke particle diameter. Numerous numerical studies (Nogami *et al.*, 2004; Gupta and Rudolph, 2006; Selvarasu *et al.*, 2006; Rangarajan *et al.*, 2014) also confirm this observation.

Furthermore, an inspection of the coke velocities shown in Fig. 13 suggests that the formation of the raceway does not change the bed structure very much, i. e., the raceway is quite localized; particles in the bed can adjust themselves in response to the disturbance. Such a phenomenon has also been observed experimentally and was confirmed by numerical calculations using the DEM approach (Xu *et al.*, 2000; Goto *et al.*, 2002; Xu, 2003; Feng *et al.*, 2003; Nogami *et al.*, 2004; Yuu *et al.*, 2005; Umekage *et al.*, 2007; Zhu *et al.*, 2011; Hilton and Cleary, 2012; Adema, 2014).

Numerical models for raceway formation are complex and computationally demanding. Although, they capture various aspects of process behavior in a multidimensional frame-

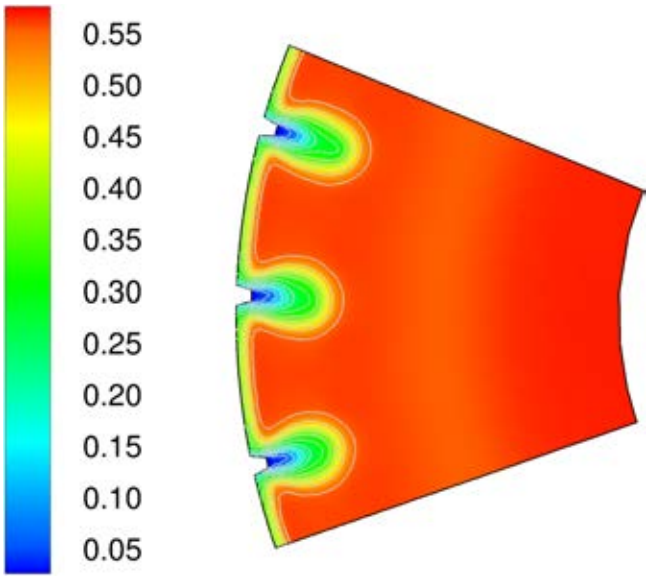

Figure 9: Spatial distribution of the granular phase volume fraction α_s for the inlet velocity $\vec{U}_{g,in} = 180\,m\,s^{-1}$ and the coke particle size $d_s = 0.038\,m$ (tuyere level)

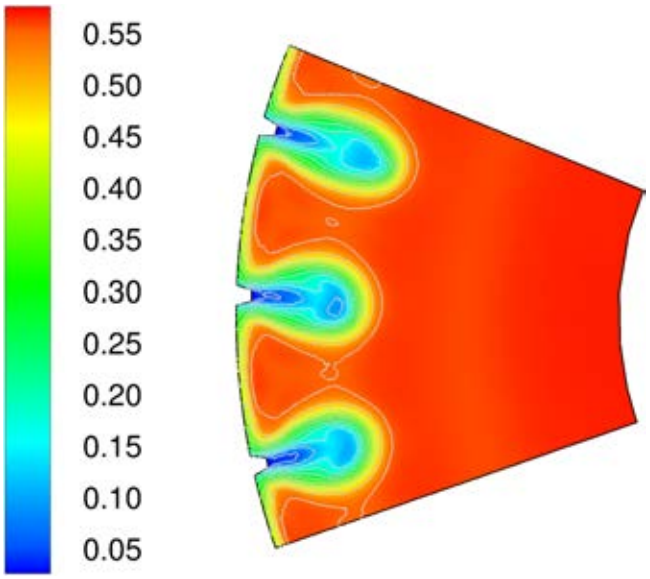

Figure 10: Spatial distribution of the granular phase volume fraction α_s for the inlet velocity $\vec{U}_{g,in} = 300\,m\,s^{-1}$ and the coke particle size $d_s = 0.038\,m$ (tuyere level)

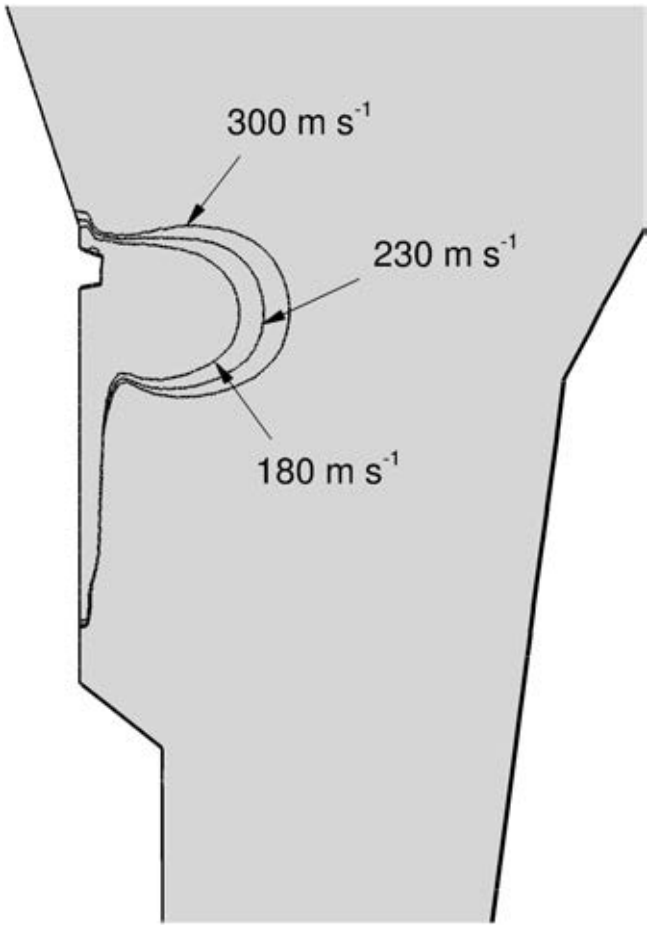

Figure 11: Shape and size of raceway zone for the coke particle size $d_s = 0.038\,m$ and different inlet velocities $\vec{U}_{g,in}$ (axial cross-section)

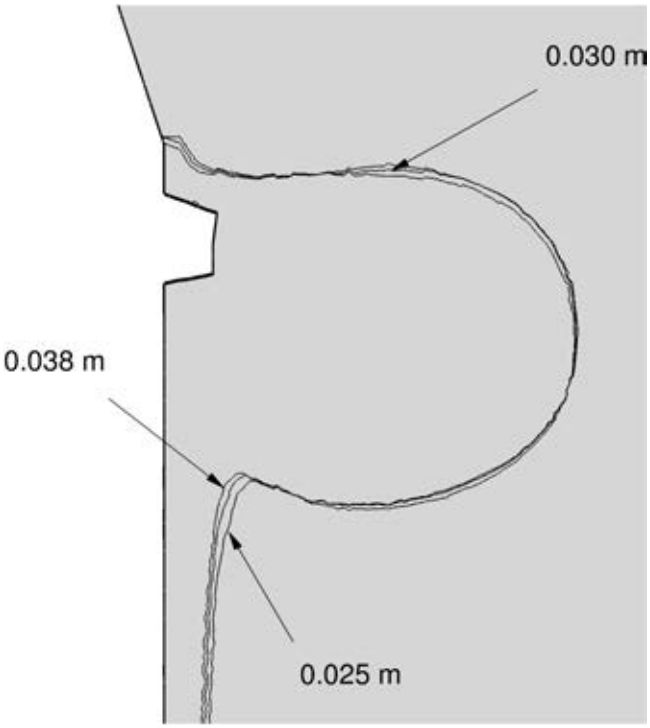

Figure 12: Shape and size of raceway zone for the inlet velocity $\vec{U}_{g,in} = 230\,m\,s^{-1}$ and different coke particle size d_s (axial cross-section)

work, the approach is not suitable for real-time application due to its long computational time. In order to make process models amenable for real-time application, it becomes imperative to minimize the computational time significantly such that the real-time predictions can be made in synchronization with the plant operational data. For such applications, reduced-order models of the blast furnace processes need to be implemented in a real-time mode, which can be synchronized with the distributed control system (DCS) for an operating blast furnace. As discussed above, the reduced-order models for predicting raceway size and shape are primarily based on force and momentum balance and incorporate semi-empirical formalism to capture the process behavior without sacrificing the important phenomenology.

In this work the approach by Nomura (Nomura, 1986) was used. The predefined geometry of the raceway is described by using its depth, D_{rw}, width, W_{rw}, and height, H_{rw}, which are determined from a force balance formulated for two different points on the surface of the raceway boundary. The resulting correlation for the depth, width, and height of the raceway are

$$\frac{D_{\mathrm{rw}}}{D_{\mathrm{tuyere}}} = C_1 \left[\rho_{\mathrm{g},0} \left(\frac{\dot{V}_{\mathrm{g},0}}{S_{\mathrm{tuyere}}} \right)^2 \frac{p_0}{p} \frac{T_{\mathrm{g}}}{T_0} \frac{1}{\vec{g}\, d_{\mathrm{s}}\, \rho_{\mathrm{s}}} \right]^{C_2}, \tag{32}$$

$$\frac{W_{\mathrm{rw}}}{D_{\mathrm{tuyere}}} = C_3 \left(\frac{D_{\mathrm{rw}}}{D_{\mathrm{tuyere}}} \right)^{C_4}, \tag{33}$$

$$\frac{\left(4H_{\mathrm{rw}}^2 + D_{\mathrm{rw}}^2\right) W_{\mathrm{rw}}}{H_{\mathrm{rw}}\, D_{\mathrm{tuyere}}^2} = C_5 \left(\frac{D_{\mathrm{rw}}}{D_{\mathrm{tuyere}}} \right)^{C_6}. \tag{34}$$

In the work of Nomura (Nomura, 1986) the model parameters C_1, C_2, …, C_6 are determined by using a comprehensive set of experimental data including data from other researchers as well as own data for different industrial-scale BFs. In order to achieve better approximation for the BF geometry under consideration the model parameters can be redefined using numerical data discussed above.
Figs. 14 and 15 show the resulting raceway dimensions as functions of the operational parameters for the newly defined set of model parameters. The new model parameters are summarized in Table 4.

Table 4: Model parameters for semi-empirical relations

C_1	C_2	C_3	C_4	C_5	C_6
1.8	0.275	0.45	1.34	1.4	2.18

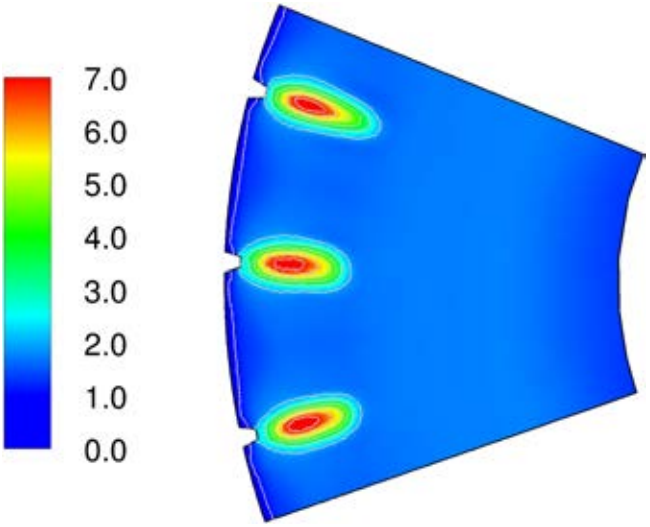

Figure 13: Spatial distribution of the granular phase velocity $\vec{U}_{\mathrm{s}}$ for the inlet velocity $\vec{U}_{\mathrm{g,in}} = 300\,\mathrm{m\,s^{-1}}$ and the coke particle size $d_{\mathrm{s}} = 0.038\,\mathrm{m}$ (tuyere level)

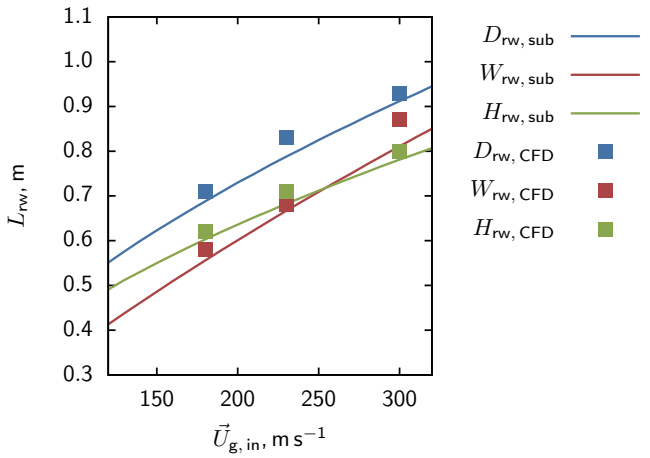

Figure 14: Dimensions of the raceway zone as a function of the gas inlet velocity for $d_{\mathrm{s}} = 0.038\,\mathrm{m}$

CONCLUSION

The shape and size of the raceway zone of an industrial-scale blast furnace have been numerically predicted in the Eulerian-Eulerian frame of reference for different blast velocities and coke particle sizes. The major observations are:

- An increase in the blast velocity increases the size of the raceway zone and the interaction with the neighbor ones.
- Increasing the size of the coke particles leads to decreasing of the raceway zone mainly due to the different mass-to-surface ratio of the coke particles.
- The real-time prediction of the shape and size of the raceway zone can be implemented using semi-empirical models based on force balance.

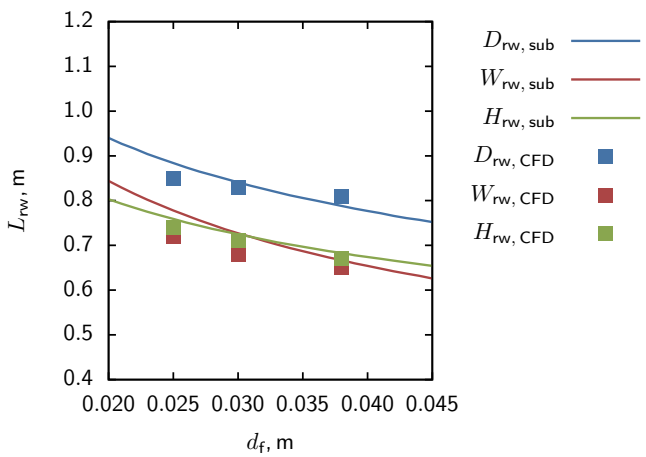

Figure 15: Dimensions of the raceway zone as a function of the coke particle size for $\vec{U}_{\mathrm{g,in}} = 230\,\mathrm{m\,s^{-1}}$

ACKNOWLEDGEMENT

This research has been funded by ArcelorMittal Eisenhüttenstadt GmbH and ArcelorMittal Bremen GmbH. The authors gratefully acknowledge the financial support.

REFERENCES

ADEMA, A. (2014). *DEM-CFD modelling of the ironmaking blast furnace*. Ph.D. thesis, Delft University of Technology.

AOKI, H., NOGAMI, H., TSUGE, H., MIURA, T. and FURUKAWA, T. (1993). "Simulation of transport phenomena around the raceway zone in the blast furnace with and without pulverized coal injection". *ISIJ International*, **33(6)**, 646–654.

CSANADY, G.T. (1963). "Turbulent diffusion of heavy particles in atmosphere". *Journal of the Atmospheric Sciences*, **20**, 201–208.

DE BERTODANO, M.L. (1991). *Turbulent bubbly flow in a triangular duct*. Ph.D. thesis, Rensselaer Polytechnic Institute, Troy, New York.

DING, J. and GIDASPOW, D. (1990). "A bubling fluidization model using kinetic theory of granular flow". *AIChE Journal*, **36**, 523–538.

ELGOBASHI, S.E. and ABOU, T.W. (1983). "A two equation turbulence model for two phase flows". *Physics of Fluids*, **26**, 931–938.

ERGUN, S. (1952). "Fluid flow through packed columns". *Chemical Engineering Progress*, **48(2)**, 89–94.

FENG, Y.Q., PINSON, D., YU, A.B., CHEW, S.J. and ZULLI, P. (2003). "Numerical study of gas–solid flow in the raceway of a blast furnace". *Steel Research International*, **74(9)**, 523–530.

FERZIGER, J. and PERIć, M. (2002). *Computational Methods for Fluid Dynamics*. 3rd ed. Springer, Berlin.

FLINT, P.J. and BURGESS, J.M. (1992). "A fundamental study of raceway size in two dimensions". *Metallurgical transacions B*, **23B**, 267–283.

GEERDES, M., CHAIGNEAU, R., KURUNOV, I., LINGIARDI, O. and RICKETTS, J. (eds.) (2015). *Modern Blast Furnace Ironmaking: An Introduction*. 3rd ed. IOS Press, Netherlands.

GIDASPOW, D. (1994). *Multiphase Flow and Fluidization: Continuum and Kinetic Theory Descriptions*. Academic Press, Boston.

GIDASPOW, D., BEZBURUAH, R. and DING, J. (1992). "Hydrodynamics of circulating fluidized beds: Kinetic theory approach". *Proceedings of the 7th Engineering Foundation Conference on Fluidization*, 75–82. Brisbane, Australia.

GOTO, K., MURAI, R., MURAO, A., SATO, M., ASANUMA, M. and ARIYAMA, T. (2002). "Massive combustion technology of solid fuel injected into blast furnace". *International Blast Furnace Lower Zone Symposium*, 1. Australasian Institute of Mining and Metallurgy (AusIMM), Wollongong, Australia.

GUPTA, G.S. (2005). "Prediction of cavity size in the packed bed systems using new correlations and mathematical model". International Application Published under the Patent Cooperation Treaty (PCT). International Publication Number: WO 2005/010218 A1.

GUPTA, G.S. and RUDOLPH, V. (2006). "Comparison of blast furnace raceway size with theory". *ISIJ International*, **46(2)**, 196–201.

HELLBERG, P., JONSSON, T.L.I., JöNSSON, P.G. and SHENG, D.Y. (2005). "A model of gas injection into a blast furnace tuyere". *Fourth International Conference on CFD in the Oil and Gas, Metallurgical & Process Industries*, 1–5. SINTEF/NTNU.

HILTON, J.E. and CLEARY, P.W. (2012). "Raceway formation in laterally gas-driven particle beds". *Chemical Engineering Science*, **80**, 306–316.

HUILIN, L., GIDASPOW, D., BOUILLARD, J. and WENTIE, L. (2003). "Hydrodynamic simulation of gas–solid flow in a riser using kinetic theory of granular flow". *Chemical Engineering Journal*, **95**, 1–13.

LAUNDER, B.E. and SPALDING, D.B. (1972). *Lectures in Mathematical Models of Turbulence*. Academic Press, London, England.

LAUNDER, B.E. and SPALDING, D.B. (1974). "The numerical computation of turbulent flows". *Computer Methods in Applied Mechanics and Engineering*, **3(2)**, 269–289.

LUN, C.K.K., SAVAGE, S.B., JEFFREY, D.J. and CHEPURNIY, N. (1984). "Kinetic theory for granular flow, inelastic particles in Couette flow and slightly inelastic particles in a general flow field". *Journal of Fluid Mechanics*, **140**, 223–56.

MONDAL, S.S., SOM, S.K. and DASH, S.K. (2005). "Numerical predictions on the influences of the air blast velocity, initial bed porosity and bed height on the shape and size of raceway zone in a blast furnace". *Journal of Physics D: Applied Physics*, **38**, 1301–1307.

NATSUI, S., NOGAMI, H., UEDA, S., KANO, J., INOUE, R. and ARIYAMA, T. (2011). "Simultaneous three-dimensional analysis of gas–solid flow in blast furnace by combining discrete element method and computational fluid dynamics". *ISIJ International*, **51(1)**, 41–50.

NOGAMI, H., YAMAOKA, H. and TAKATANI, K. (2004). "Raceway design for the innovative blast furnace". *ISIJ International*, **44**, 2150–2158.

NOMURA, S. (1986). "A simple treatment on the geometry of raceway zone". *Transactions ISIJ*, **26**, 107–113.

OHNO, Y., FURUKAWA, T. and MATSU-URA, M. (1994). "Combustion behavior of pulverized coal in a raceway cavity of blast furnace and its application to a large amount injection". *ISIJ International*, **34(8)**, 641–648.

RAJNEESH, S., SARKAR, S. and GUPTA, G.S. (2004). "Prediction of raceway size in blast furnace from two dimensional experimental correlations". *ISIJ International*, **44(8)**, 1298–1307.

RANGARAJAN, D., SHIOZAWA, T., SHEN, Y., CURTIS, J.S. and YU, A. (2014). "Influence of operating parameters on raceway properties in a model blast furnace using a two-fluid model". *Industrial & Engineering Chemistry Research*, **53**, 4983–4990.

SCHAFFER, D.G. (1987). "Instability in the evolution equations describing incompressible granular flow". *Journal of Differential Equations*, **66(19–50)**.

SELVARASU, N., GU, M., ZHOU, C. and ZHAO, Y. (2007). "Computer modeling of blast furnace raceway formation kinetics". *Proceedings of the Iron and Steel Technology Conference*, vol. 1, 425–433. Association for Iron & Steel Technology AISTech.

SELVARASU, N.K., HUANG, D., CHEN, Z., GU, M., ZHAO, Y., CHAUBAL, P. and ZHOU, C.Q. (2006). "Prediction of raceway in a blast furnace". *Proceedings of IMECE2006*, 297–303. ASME, ASME. 2006 ASME International Mechanical Engineerung Congress and Exposition.

SIMONIN, C. and VIOLLET, P.L. (1990). "Predictions of an oxygen droplet pulverization in a compressible subsonic co-flowing hydrogen flow". *Numerical Methods for Multiphase Flows, FED'91*, 65–82.

SINGH, V., GUPTA, G.S. and RAJNEESH, S. (2006). "Modelling of void initiation and breaking phenomena in a packed bed". *Ironmaking and Steelmaking*, **33(2)**, 101–110.

SZEKELY, J. and POVEROMO, J.J. (1975). "A mathematical and physical representation of the raceway region in the iron blast furnace". *Metallurgical Transactions B*, **6B**, 119–130.

UMEKAGE, T., KADOWAKI, M. and YUU, S. (2007). "Numerical simulation of effect of tuyere angle and wall scaffolding on unsteady gas and particle flows including raceway in blast furnace". *ISIJ International*, **47(5)**, 659–668.

VDE (1976). "Automatisierung des Hochofenverfahrens, Teil 2: Modelluntersuchungen über die Ausbildung der Zirkulationszone vor den Blasformen von Hochöfen". Tech. rep., Kommission der Europäischen Gemeinschaften, Düsseldorf.

WEN, C.Y. and YU, Y.H. (1966). "Mechanics of fluidization". *Chemical Engineering Progress Symposium Series*, vol. 62, 100–111.

XU, B.H. (2003). "Modelling of the gas fluidization of a mixture of cohesive and cohesionless particles by a combined continuum and discrete model". *KONA Powder and Particle Journal*, **21**, 100–108.

XU, B.H., YU, A.B., CHEW, S.J. and ZULLI, P. (2000). "Numerical simulation of the gas–solid flow in a bed with lateral gas blasting". *Powder Technology*, **109**, 13–26.

YUU, S., UMEKAGE, T. and MIYAHARA, T. (2005). "Prediction of stable and unstable flows in blast furnace raceway using numerical simulation methods for gas and particles". *ISIJ International*, **45(10)**, 1406–1415.

YUU, S., UMEKAGE, T., MATSUZAKI, S., KADOWAKI, M. and KUNITOMO, K. (2010). "Large scale simulation of coke and iron ore particle motions and air flow in actual blast furnace". *ISIJ International*, **50(7)**, 962–971.

ZHU, H.P., ZHOU, Z.Y., HOU, Q.F. and YU, A.B. (2011). "Linking discrete particle simulation to continuum process modelling for granular matter: Theory and application". *Particuology*, **9**, 342–357.